

## Study of the in medium cross-section and of the clustering process by means of the Bayesian technique applied to a nuclear reaction at Fermi energy

S. PIANTELLI<sup>(1)</sup>, A. CAMAIANI<sup>(2)</sup>(<sup>1</sup>), G. POGGI<sup>(2)</sup>(<sup>1</sup>), A. ONO<sup>(3)</sup>, C. FROSIN<sup>(2)</sup>(<sup>1</sup>), L. BALDESI<sup>(2)</sup>(<sup>1</sup>), S. BARLINI<sup>(2)</sup>(<sup>1</sup>), B. BORDERIE<sup>(4)</sup>, R. BOUGAULT<sup>(5)</sup>, G. CASINI<sup>(1)</sup>, C. CIAMPI<sup>(6)</sup>, M. CICERCHIA<sup>(7)</sup>(<sup>8</sup>), A. CHBIHI<sup>(6)</sup>, D. DELL'AQUILA<sup>(9)</sup>(<sup>10</sup>), J. A. DUENÑAS<sup>(25)</sup>, Q. FABLE<sup>(24)</sup>, D. FABRIS<sup>(8)</sup>, J. D. FRANKLAND<sup>(6)</sup>, T. GÉNARD<sup>(6)</sup>, D. GRUYER<sup>(5)</sup>, M. HENRI<sup>(11)</sup>, B. HONG<sup>(12)</sup>(<sup>13</sup>), M. J. KWEON<sup>(14)</sup>, S. KIM<sup>(15)</sup>, A. KORDYASZ<sup>(16)</sup>, T. KOZIK<sup>(17)</sup>, I. LOMBARDO<sup>(18)</sup>(<sup>19</sup>), O. LOPEZ<sup>(5)</sup>, T. MARCHI<sup>(24)</sup>, K. MAZUREK<sup>(20)</sup>, S. H. NAM<sup>(12)</sup>(<sup>13</sup>), J. LEMARIÉ<sup>(6)</sup>, N. LE NEINDRE<sup>(5)</sup>, P. OTTANELLI<sup>(21)</sup>, M. PARLOG<sup>(5)</sup>(<sup>22</sup>), J. PARK<sup>(12)</sup>(<sup>13</sup>), G. PASQUALI<sup>(2)</sup>(<sup>1</sup>), A. REBILLARD-SOULIÉ<sup>(5)</sup>, B. H. SUN<sup>(23)</sup>, A. A. STEFANINI<sup>(2)</sup>(<sup>1</sup>), S. TERASHIMA<sup>(23)</sup>, S. UPADHYAYA<sup>(17)</sup>, S. VALDRÉ<sup>(1)</sup>, G. VERDE<sup>(19)</sup>, E. VIENT<sup>(5)</sup> and M. VIGILANTE<sup>(9)</sup>(<sup>10</sup>)

<sup>(1)</sup> INFN, Sezione di Firenze - Firenze, Italy

<sup>(2)</sup> Dipartimento di Fisica, Università di Firenze - Firenze, Italy

<sup>(3)</sup> Department of Physics, Tohoku University - Sendai 980-8578, Japan

<sup>(4)</sup> Université Paris-Saclay, CNRS/IN2P3, IJCLab - 91405 Orsay, France

<sup>(5)</sup> Normandie Université, ENSICAEN, UNICAEN, CNRS/IN2P3, LPC Caen 14000 Caen, France

<sup>(6)</sup> Grand Accélérateur National d'Ions Lourds (GANIL), CEA/DRF-CNRS/IN2P3 Boulevard Henri Becquerel, 14076 Caen, France

<sup>(7)</sup> Dipartimento di Fisica, Università di Padova - Padova, Italy

<sup>(8)</sup> INFN, Sezione di Padova - Padova, Italy

<sup>(9)</sup> Dipartimento di Fisica, Università di Napoli - Napoli, Italy

<sup>(10)</sup> INFN, Sezione di Napoli - Napoli, Italy

<sup>(11)</sup> CEA/INSTN/UECC - 50130 Cherbourg-Octeville, France

<sup>(12)</sup> Center for Extreme Nuclear Matters (CENuM), Korea University - Seoul 02841, Republic of Korea

<sup>(13)</sup> Department of Physics, Korea University - Seoul 02841, Republic of Korea

<sup>(14)</sup> Department of Physics, Inha University - Incheon 22212, Republic of Korea

<sup>(15)</sup> Institute for Basic Science - Daejeon 34126, Republic of Korea

<sup>(16)</sup> Heavy Ion Laboratory, University of Warsaw - 02-093 Warszawa, Poland

<sup>(17)</sup> Faculty of Physics, Astronomy and Applied Computer Science, Jagiellonian University 30-348 Krakow, Poland

<sup>(18)</sup> Dipartimento di Fisica, Università di Catania - Catania, Italy

<sup>(19)</sup> INFN, Sezione di Catania - Catania, Italy

<sup>(20)</sup> Institute of Nuclear Physics Polish Academy of Sciences - Radzikowskiego 152, 31-342 Krakow, Poland

<sup>(21)</sup> INFN, Sezione di Pisa - Pisa, Italy

<sup>(22)</sup> National Institute of Physics and Nuclear Engineering (IFIN-HH) - RO-077125 Bucharest Magurele, Romania

<sup>(23)</sup> School of Physics and Nuclear Energy Engineering, Beihang University - Beijing 100191, China

<sup>(24)</sup> Laboratoire des 2 Infinis, Toulouse (L2IT-IN2P3), Université de Toulouse, CNRS, UPS F-31062 Toulouse Cedex 9, France

<sup>(25)</sup> Departamento de Ingeniería Eléctrica y Centro de Estudios Avanzados en Física, Matemáticas y Computación, Universidad de Huelva - 21007 Huelva, Spain

received 26 November 2024

**Summary.** — A Bayesian analysis aimed at tuning two parameters of the AMD model, one of them related to the in medium nucleon nucleon cross-section and the other to the clustering, has been performed. Experimental data collected with four blocks of the FAZIA setup have been compared with simulated data built with different values of the investigated parameters.

## 1. – Introduction

It is well known that the theoretical description of heavy ion collisions in the intermediate energy regime (20–100 MeV/nucleon) is a challenge because in this region in medium effects and nucleon nucleon collisions coexist. A reasonable description can be obtained with modern transport models, which belong to two main classes: BNV-type models, describing the time evolution of one-body density, and molecular dynamics models, where nucleons are treated as wavepackets. In this work we focused on the dynamical model AMD [1,2], which was able to describe the main properties of heavy ion collisions in the intermediate region in the whole impact parameter range [3-10]. In particular, we aimed at tuning two parameters of the model, one related to the in medium nucleon nucleon cross-section and one to the clustering by means of a Bayesian approach. The experimental data collected with four FAZIA blocks on the system  $^{20}\text{Ne} + ^{12}\text{C}@50\text{ MeV/nucleon}$ , *i.e.*, the same dataset discussed in [9], have been compared with simulated data produced by AMD with different values of the investigated parameters; the dynamical calculation was stopped at 500 fm/c producing about 6000 primary events and the primary ejectiles were transferred to the HF1 code [11,12] to be statistically de-excited, producing 10 secondary events for each primary one; a software replica of the setup was then applied to the produced events.

In the Bayesian approach the posterior distribution of a parameter of the model can be calculated starting from a prior distribution and from the likelihood function obtained comparing the model results as a function of the parameter distribution with the experimental observables, which, in our case, are energy and angular distributions, isotopic yields and particle multiplicities. In our analysis distributions are replaced by the first three moments, while for particle multiplicities only the mean values are considered. The likelihood  $L_j(\{p_i\})$  for each considered observable  $j$  as a function of the simulation parameters  $\{p_i\}$  has been calculated as

$$(1) \quad L_j(\{p_i\}) = e^{-\frac{1}{2}\chi_j^2(\{p_i\})}.$$

For each observable  $j$  the cumulative  $\chi^2$  is defined as

$$(2) \quad \chi_j^2(\{p_i\}) = \sum_{k=1}^3 \left[ \frac{\Lambda_{i,j}^{exp} - \Lambda_{i,j}^{mod}(\{p_i\})}{\sigma_{j,i}} \right]^2,$$

where  $\Lambda_{i,j}^{exp}$  is the  $i$ -th momentum for the experimental distribution associated to the observable  $j$ ,  $\Lambda_{i,j}^{mod}(\{p_i\})$  is the same momentum of the simulated distribution obtained when the simulation parameters are set to the values  $(\{p_i\})$ . The uncertainty  $\sigma_{j,k}$  is calculated as

$$(3) \quad \sigma_{j,i} = \sqrt{(\sigma_{j,i}^{mod})^2 + (\sigma_{j,i}^{exp})^2},$$

where  $\sigma_{j,i}^{exp(mod)}$  is the error associated to the  $i$ -th moment of the experimental (model) distribution.

The total likelihood for all the considered observables (total number  $N_o$ ) as a function of the simulation parameter values is calculated as

$$(4) \quad L^T(\{p_i\}) = \prod_{j=1}^{N_o} L_j(\{p_i\}).$$

The two parameters we investigated are:

i) the screening parameter  $\eta$  entering in the nucleon nucleon cross-section describing the collisions between nucleons or light clusters which may end with the formation of a cluster state:

$$(5) \quad \frac{d\sigma(C_1, C_2)}{d\Omega} = P(C_1, C_2, p_f, \Omega) \frac{1}{v_i} \frac{p_f}{v_f} |M|^2 p_f,$$

where  $(C_1, C_2)$  is a specific configuration for the two nucleon collision; the matrix element  $|M|^2$  for the two nucleon scattering is proportional to  $\sigma = \sigma_0 \tanh(\frac{\sigma_{free}}{\sigma_0})$ , where  $\sigma_0 = \eta \rho^{-2/3}$  [13];  $\rho$  is the nuclear density and  $\sigma_{free}$  is the free cross-section, which depends on the collision energy;  $v_i$  is the initial relative velocity between the colliding nucleons;  $p_f$  is the relative momentum vector after the momentum transfer between the two nucleons;  $v_f = \partial E / \partial p_f$ , where  $E$  is the energy of the system including the effective interaction. We want to stress that, even for large values of  $\eta$ , *i.e.*, for  $\sigma$  approaching  $\sigma_{free}$ , the differential nucleon nucleon cross-section  $\frac{d\sigma(C_1, C_2)}{d\Omega}$  of eq. (5) does not approach the free nucleon nucleon cross-section. However, for larger values of  $\eta$  a larger number of nucleon nucleon collisions are allowed within AMD.

ii) A parameter  $\Gamma$  reducing the  $P(C_1, C_2, p_f, \Omega)$  factor, which is the overlap probability between the wave functions of the colliding nucleons for the cluster formation.  $\Gamma = 0$  means that the cluster formation is not allowed, while  $\Gamma = \infty$  means maximum probability of cluster formation.

Concerning the prior distribution, we assumed a flat distribution between  $\Gamma = 0$  and  $\infty$  for the clustering parameter and a Gaussian centered around  $\eta = 0.85$  for the screening parameter and ranging from  $\eta = 0.15$  up to  $\eta = 5$ , *i.e.*, close to the free cross-section for  $\sigma$ ;  $\eta = 0.85$  is the value used in all the previous comparisons between AMD results and FAZIA experimental data. In [9] it was shown that  $\Gamma = \infty$  gives better results in terms of reproducing the experimental data than  $\Gamma = 0$ .

## 2. – Test of the method

Before applying the technique to the experimental data, a test was performed aiming at validating the procedure. A particular simulation, the one with  $\eta = 0.55$  and  $\Gamma =$

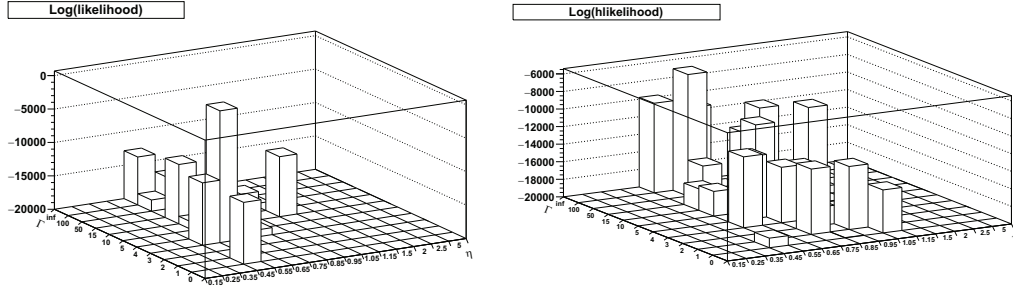


Fig. 1. – Left: logarithm of the likelihood distribution as a function of  $\eta$  and  $\Gamma$  parameters obtained assuming as experimental data the simulation with  $\eta = 0.55$  and  $\Gamma = 4$ , including in the calculation all the available observables. Right: logarithm of the likelihood distribution as a function of  $\eta$  and  $\Gamma$  parameters obtained assuming as experimental data the simulation with  $\eta = 0.55$  and  $\Gamma = 4$  and GEMINI++ as afterburner, including in the calculation all the available observables.

4, was used as “experimental” data and the whole Bayesian procedure was applied, including all the available observables. A correct working should result in a likelihood distribution peaked at  $\eta = 0.55$  and  $\Gamma = 4$ ; the obtained result, as shown in fig. 1 (left), are in agreement with this expectation, thus evidencing the regularity of the applied procedure.

Another aspect to evaluate is the stability of the result when the afterburner is changed; this can be done for example assuming as “experimental” simulation the one with  $\eta = 0.55$  and  $\Gamma = 4$  but with GEMINI++ [14] as afterburner, while the likelihood is calculated starting from simulations where the afterburner is HF1. The obtained results are shown in fig. 1 (right) for the likelihood; it can be noted that the absolute maximum is shifted with respect to the correct one; in fact the absolute maximum is located at  $\eta = 0.65$  and  $\Gamma = 100$ . However, a secondary maximum can be seen at the original value.

This result confirms, as expected, that there is a strong influence of the afterburner on the secondary distributions of the observables and that the afterburners, despite being implementations of the statistical model for the decay of the compound nucleus, are not equivalent; therefore it is important to keep in mind that what we are testing with the adopted technique is not the dynamical model only, but the pair AMD plus HF1.

### 3. – Results

In a first attempt, all the available observables have been included in the analysis, *i.e.*, the charge and angular distribution, particle multiplicities, isotopic distributions. The obtained result for the logarithm of the posterior distribution as a function of  $\eta$  and  $\Gamma$  parameters is shown in fig. 2. A maximum overcoming of more than 10% all the other values can be seen in the picture in correspondence of  $\eta = 2.5$  and  $\Gamma = 100$ . The position of the maximum is the same also in the likelihood distribution. This result confirms the fact that the introduction of the clustering process is mandatory to reproduce the experimental data, as already stated in [9]. Here we point out that a  $\sigma$  value closer to the free one ( $\eta = 2.5$ ) with respect to the standard value of  $\eta = 0.85$  previously used in the comparison between AMD and FAZIA data seems to improve the reproduction of the experimental data.

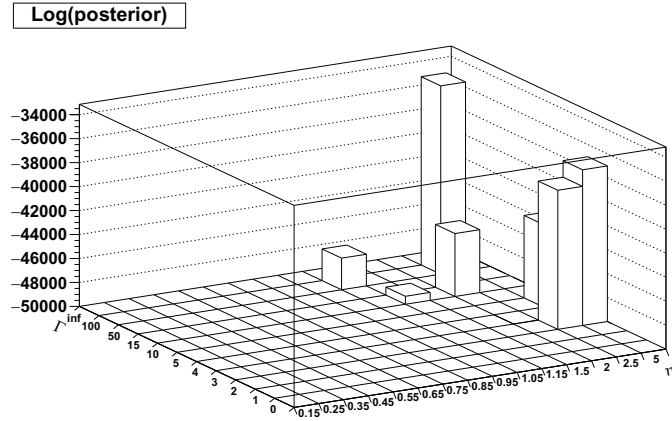


Fig. 2. – Logarithm of the posterior distribution as a function of  $\eta$  and  $\Gamma$  parameters obtained including all the available observables.

In order to check the stability of the obtained result, we reduced the dataset of observables adopted for the Bayesian inference. If the investigated observables are restricted to those showing the largest sensitivity to the switching on and off of the clustering ( $\Gamma = \infty$  *vs.*  $\Gamma = 0$ ), as shown in [9], the obtained posterior distribution is shown in fig. 3. In this picture the included observables are the energy and angular distributions of p, d, t,  $^3\text{He}$ ,  $\alpha$ ,  $^6\text{Li}$ ,  $^7\text{Be}$ ,  $^{10}\text{B}$ . Again, the maximum of the posterior distribution is located in the top right part of the  $(\Gamma, \eta)$ -plane, but its position is slightly shifted with respect to the case of fig. 2. The  $\sigma$  value is closer to the free one ( $\eta = 5$ ) and  $\Gamma = 15$  means a partial reduction of the clustering process.

As an example of the sensitivity to the  $\Gamma$  and  $\eta$  parameters, in fig. 4 the energy and centre of mass angular distributions for protons and  $\alpha$  particles are shown; experimental data (symbols) are compared to the simulated ones obtained with  $\eta = 5$  and  $\Gamma = 15$  (black dashed lines), with  $\eta = 2.5$  and  $\Gamma = 100$  (blue continuous line) and with the standard simulation with  $\eta = 0.85$  and  $\Gamma = \infty$  usually used to compare with the experimental

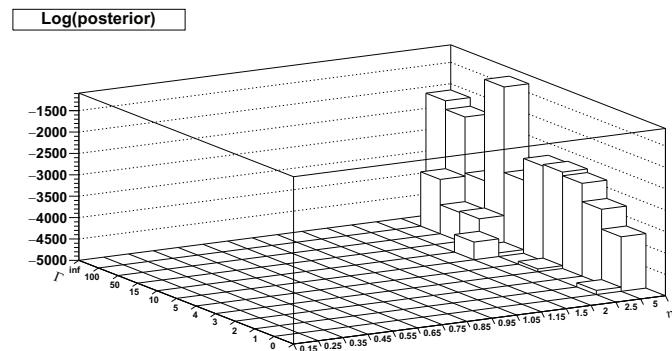


Fig. 3. – Logarithm of the posterior distribution as a function of  $\eta$  and  $\Gamma$  parameters obtained including only some observables (see text).

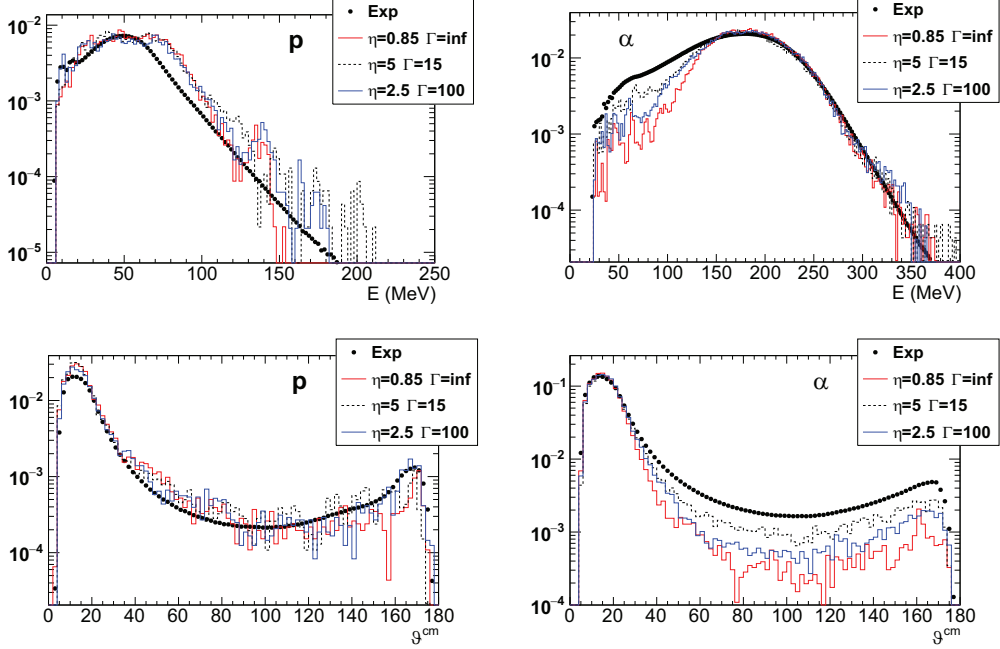


Fig. 4. – Top left: lab kinetic energy distribution of protons; top right: lab kinetic energy of  $\alpha$ ; bottom left: c.m. polar angle distribution for protons; bottom right: c.m. polar angle distributions for  $\alpha$ . In all panels symbols are experimental data, the dashed black histogram corresponds to the simulation with  $\Gamma = 15$  and  $\eta = 5$ ; the blue histogram corresponds to the simulation with  $\Gamma = 100$  and  $\eta = 2.5$ , while the red histogram is the standard simulation with  $\Gamma = \infty$  and  $\eta = 0.85$ .

data of FAZIA (red lines). The black dashed lines correspond to the maximum of the posterior distribution shown in fig. 3, *i.e.*, the one obtained including only a limited dataset of observables, while the blue continuous line corresponds to the maximum of the posterior distribution obtained including all the observables (see fig. 2). A clear improvement in the quality of the agreement is observed for  $\alpha$  particles when moving from the standard simulation to the one corresponding to the maximum of the likelihood (especially for the reduced dataset of observables), while no evident changes are found for protons.

#### 4. – Summary and conclusions

Some preliminary results concerning a Bayesian analysis aimed at estimating two parameters of the AMD model, one related to the clustering and one to the in-medium NN cross-section, were shown. The obtained results depend both on the chosen afterburner and on the considered observables. However, a trend towards the upper right region of the  $(\eta, \Gamma)$ -plane seems to take place, provided that a consistent set of observables are included in the calculation. In fact, for some single observables better solutions can be found in different regions of the plane, but a reasonable global description requires strong clustering and cross-section  $\sigma$  close to the free one.

The adopted Bayesian analysis seems a promising tool to improve the quality of the agreement between experimental data and simulations. The drawback of the method

is the very long calculation time required to build a proper grid of simulation on a wide range of values for the different parameters, which prevents from producing a high statistics, as it would be necessary for a general reduction of the model uncertainties. A possible overcome of this problem might be the use of machine learning technique (or other approximation methods) to extrapolate the model in regions of the parameter grid not covered by the run simulations. In this way a less dense grid could be produced, improving the statistics for the effectively run simulations. This would allow to extend the technique also to heavier systems, for example those measured by the INDRA-FAZIA apparatus.

## REFERENCES

- [1] ONO A. *et al.*, *Phys. Rev. Lett.*, **68** (1992) 2898.
- [2] ONO A., *Phys. Rev. C*, **59** (1999) 853.
- [3] PIANTELLI S. *et al.*, *Phys. Rev. C*, **99** (2019) 064616.
- [4] CAMAIANI A. *et al.*, *Phys. Rev. C*, **103** (2021) 014605.
- [5] PIANTELLI S. *et al.*, *Phys. Rev. C*, **101** (2020) 034613.
- [6] PIANTELLI S. *et al.*, *Phys. Rev. C*, **103** (2021) 014603.
- [7] CIAMPI C. *et al.*, *Phys. Rev. C*, **106** (2022) 024603.
- [8] PIANTELLI S. *et al.*, *Phys. Rev. C*, **107** (2023) 044607.
- [9] FROSIN C. *et al.*, *Phys. Rev. C*, **107** (2023) 044614.
- [10] CAMAIANI A. *et al.*, *Phys. Rev. C*, **102** (2020) 044607.
- [11] BAIOTTO G. *et al.*, *Phys. Rev. C*, **87** (2013) 054614.
- [12] MORELLI L. *et al.*, *Phys. Rev. C*, **99** (2019) 054610.
- [13] COUPLAND D. D. S. *et al.*, *Phys. Rev. C*, **84** (2011) 054603.
- [14] CHARITY R. J., *Phys. Rev. C*, **82** (2010) 014610.